

Tuning Electrostatic Interactions of Colloidal Particles at Oil-Water Interfaces with Organic Salts

Carolina van Baalen[✉], Jacopo Vialetto^{✉,*}, and Lucio Isa^{✉,†}

Laboratory for Soft Materials and Interfaces, Department of Materials, ETH Zürich, Vladimir-Prelog-Weg 5, 8093 Zürich, Switzerland



(Received 4 May 2023; accepted 23 August 2023; published 19 September 2023)

Monolayers of colloidal particles at oil-water interfaces readily crystallize owing to electrostatic repulsion, which is often mediated through the oil. However, little attempts exist to control it using oil-soluble electrolytes. We probe the interactions among charged hydrophobic microspheres confined at a water-hexadecane interface and show that repulsion can be continuously tuned over orders of magnitude upon introducing nanomolar amounts of an organic salt into the oil. Our results are compatible with an associative discharging mechanism of surface groups at the particle-oil interface, similar to the charge regulation observed for charged colloids in nonpolar solvents.

DOI: [10.1103/PhysRevLett.131.128202](https://doi.org/10.1103/PhysRevLett.131.128202)

Particles adsorbed at a fluid interface are key components in multiple technological processes, from mineral recovery in froth flotation [1], to the fabrication of ordered two-dimensional (2D) materials [2]. Confinement at an interface makes it also possible to obtain model systems to study, for example, crystallization in two dimensions on planar [3–6] as well as curved surfaces [7]. Regardless of the final goal, understanding and controlling the interactions between particles in interfacial monolayers is essential to achieve the desired structural and mechanical properties. To this end, a variety of additives [8], such as salts or surfactants [9–15], and external stimuli (e.g., magnetic fields or light) [16–18] have been used to tune particle assembly, organization, and the mechanical stability of the resulting monolayers. While these phenomenological approaches result in a fine-tuning of the monolayers' properties, unraveling the precise nature of the interparticle potential still presents opportunities.

The interactions among colloidal particles confined at a fluid interface are governed by a number of forces [19–21], some of which are exclusive to the interface itself (e.g., capillary forces [22,23], interface charge [24]). Concerning electrostatic forces, several studies have shown that the particles may exhibit strong, long-range repulsive interactions that can be orders of magnitude larger than those attained in a single fluid phase [20,25–27], making these colloidal monolayers crystallize at very low packing fractions [28]. Such repulsion arises from an asymmetric dissociation of the charged groups on the particle surface in the two fluids and from the material discontinuity, i.e., different dielectric properties, across the interface. In addition to the classic DLVO screened-Coulomb term, a multipolar expansion of the field becomes necessary to fully describe the electrostatic interactions [29]. Particularly intriguing is the case of spherical hydrophobic charged colloids adsorbed at a water-nonpolar fluid

interface. In this case, several experimental techniques, (e.g., optical tweezers [30–35], microstructural investigations [34,36], collective sinking of particle monolayers [37], and compression in a Langmuir-Blodgett trough [25,38]) have repeatedly confirmed that a pairwise dipolar repulsion of the form $U(r) \propto 1/r^3$ is the dominant term in the electrostatic interaction potential U as a function of interparticle distance r .

In spite of the agreement on the functional form of the potential, different mechanisms have been proposed to describe the microscopic origins of the electrostatic dipoles, with the two main ones invoking either charge asymmetry on the aqueous side of the interface [19,29,30,39], or the presence of residual charges exposed to the oil [35,40], which remain essentially unscreened due to the very large Debye length in the nonpolar phase. Surprisingly, even though for many polystyrene latexes and hydrophobized silica particles the latter explanation seems to be more likely, the only attempts to tune the interaction potentials have been through the use of additives (e.g., salts, surfactants) to the aqueous subphase [26,34,41], or via surface modifications to change particle wettability by means of silanization [20,26]. Conversely, electrostatic interactions in bulk nonpolar solvents [42,43] and in proximity of fluid interfaces [44] have been extensively investigated together with ways to regulate them by adding organic salts or charge-regulating surfactants [42,45–47].

Inspired by those studies and addressing an opportunity to fill an apparent gap in the literature, in this Letter we show that the strength of the dipolar interparticle interaction potential at water-oil interfaces can be continuously tuned over orders of magnitude upon introducing small amounts of a charge-regulating organic salt, the ionic liquid trihexyltetradecylphosphonium decanoate, into the nonpolar phase. We extract the interaction potential by measuring the interparticle distance as a function of height in a vertical

monolayer under the action of gravity [20,26,48,49]. This method, compared to the ones mentioned above offers the advantage of a robust, reproducible, and statistically relevant measurement over thousands of particles in a simple optical setup.

We first create a macroscopically flat, horizontal water-hexadecane interface inside an experimental cell made out of two concentric glass rings glued on a glass cover slip. A schematic of the experimental cell is shown in Fig. S1, and further details of the experimental setup can be found in [50]. The inner and outer glass rings of the experimental cell have an inner diameter of 6 and 14 mm, and a height of 3 and 5 mm, respectively. The inner glass ring is filled with the aqueous phase until the surface is pinned to the edge (84 μL). Hexadecane is then pipetted on top to fill up the outer glass ring. In order to minimize the presence of surface-active contaminants, the hexadecane was purified by three times extraction through an alumina and silica gel column, and the particles cleaned by several cycles of centrifugation and supernatant exchange (See [50] for experimental details, which includes Refs. [14,51]).

We used different sulfonated polystyrene (PS) particles, with respective diameter, contact angle (See [50] for details on the measurement, which includes Ref. [39]), and zeta potential in Milli-Q water of $d = 2.80 \mu\text{m}$, $\theta = 114.5 \pm 2.5$, and $\zeta = -45.2 \pm 1.1 \text{ mV}$, $d = 2.48 \mu\text{m}$, $\theta = 106.7 \pm 4.5$, and $\zeta = -45.3 \pm 1.2 \text{ mV}$, and $d = 2.07 \mu\text{m}$, $\theta = 101.5 \pm 3.5$, and $\zeta = -35.2 \pm 1.8 \text{ mV}$, and obtained 2D, hexagonally packed monolayers (lattice spacing $\approx 7d$) by spreading 0.5 μL of a 3 : 1 surfactant-free particle suspension: isopropanol mixture directly at the interface [Fig. 1(a)]. With this spreading protocol, some of the negative charges on the particle surface arising from the dissociation of sulfonate groups are retained on the surface exposed to the oil phase when the particles are “instantly” confined at the oil-water interface, resulting in strong electrostatic repulsion and concomitant crystallization at low densities [25,52,53]. After sealing, the cell was carefully flipped by 90°, bringing the particle-loaded interface into a vertical position, and was allowed to equilibrate for at least 8 h [Fig. 1(b)]. Under gravity, a gradient in interparticle lattice spacing (r) is established as a function of height (z). [Fig. S(4)]. We imaged this gradient by localizing particles from up to 18 stitched consecutive dark-field images of $300 \times 1000 \mu\text{m}^2$, see Fig. 1(c), and assigned $z = 0 \text{ mm}$ to the uppermost particle in the monolayer. Note that the particle sedimentation length is approximately 600 nm, i.e., much smaller than d , hence all particles in the monolayer sediment and compression of the monolayer starts at the uppermost particle.

Previous reports to extract the interparticle interaction potential from the barometric density profile of a vertical particle monolayer required the numerical integration of $U(r)$ vs z [49]. However, this approach suffers from potential errors arising from the size of the integration step and several assumptions have to be made on system

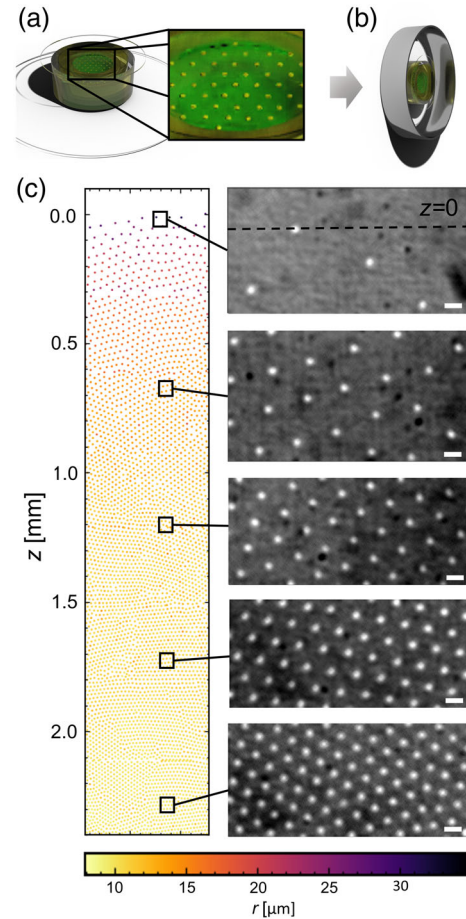


FIG. 1. Illustration of the experiments. (a) Scheme (not to scale) of the cell holding the water-hexadecane interface, with a hexagonally packed colloidal monolayer. (b) After monolayer formation, the cell is flipped by 90° and allowed to equilibrate for $> 8 \text{ h}$. (c) Representative plot of the particle position as a function of height (z) in a vertical monolayer of PS particles ($d = 2.80 \mu\text{m}$) after 15 h, and corresponding dark field microscopy images. $z = 0 \text{ mm}$ is assigned to the uppermost particle in the monolayer, as illustrated in the top dark-field image, and particles are color-coded according to their average interparticle distance r . Scale bars: 10 μm .

parameters, such as the contact angle and the packing arrangement of the particles, which contribute to another degree of variability at every integration step. Therefore, we instead directly fit the raw experimental z versus r data to measure the potential. We obtain the r and z values by dividing the whole monolayer in horizontal bins with a 50 μm height and computing the average interparticle distance and vertical position in each bin. Assuming the well-established form of the repulsive dipolar potential U at the fluid interface to follow [29]

$$\frac{U(r)}{k_B T} = a_2 \frac{1}{r^3}, \quad (1)$$

it is straightforward to derive that the raw z vs r data must obey [50]

$$z(r) = A_2 \frac{1}{r^3} + C_2, \quad (2)$$

where C_2 is an integration constant, and A_2 relates to the prefactor a_2 commonly used in literature [31–34,41] as

$$a_2 = \frac{A_2 m^* g}{k_B T}, \quad (3)$$

where g is the gravitational constant, k_B is the Boltzmann constant, and T the absolute temperature.

Figure 2 shows a plot of z vs r for the different PS particles we used (the reproducibility of the z vs r profile is shown in Fig. S5 [50]). Starting with the $d = 2.80 \mu\text{m}$ particles (gray circles), using Eq. (2) we find an amplitude $A_2 = 1.1 \times 10^7 \pm 7.5 \times 10^4 \mu\text{m}^4$ (Table S1), corresponding to a value of $a_2 = 6.7 \times 10^{-12} \pm 4.6 \times 10^{-14} \text{m}^3$. This value is on the higher end of the literature values, i.e., ranging from 5.0×10^{-14} to $1.2 \times 10^{-12} \text{m}^3$, as observed by other groups using optical tweezers [32,33,41], or a combination of optical tweezers and other analysis techniques [34]. Notably, we calculate a_2 from multibody interactions acting in the monolayer, and in the absence of any assumption on system parameters, other than hexagonal packing. The same procedure applied to the other two samples shows that the $d = 2.48 \mu\text{m}$ particles behave very similarly to the previous ones (dark green squares), in line with the fact that they have a similar size, zeta potential, and contact angle (see Fig. S3 [50]), while the smaller $d = 2.07 \mu\text{m}$ particles (light green diamonds) retain the same $z \propto 1/r^3$ dependence, albeit with $a_2 = 5.8 \times 10^{-13} \pm 3.9 \times 10^{-15} \text{m}^3$, which is well within the range reported by the previously mentioned works.

Having benchmarked the interactions for the native particle systems, we move on to investigating the effect of additives to tune the electrostatic potential. In agreement

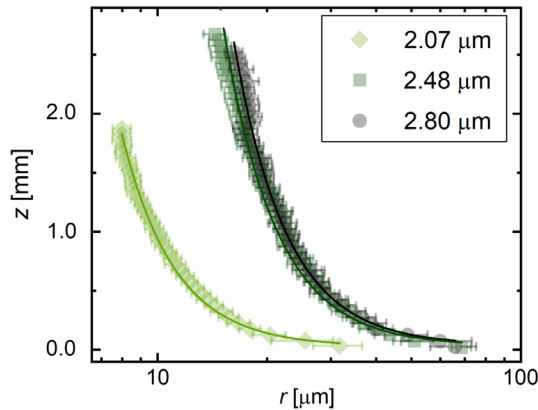


FIG. 2. Particle vertical position z versus interparticle distance r . Data for three sets of PS particles, showing the mean r in $50 \mu\text{m}$ -high horizontal bins. The error bars indicate the standard deviation of the interparticle distance. Solid lines represent the fits to Eq. (2).

with the literature [35,41,49,54], we detected only a minor effect upon addition of ionic species (sodium chloride, NaCl) to the aqueous subphase (Fig. S6 [50]). The addition of up to $0.3M$ of NaCl did not modify the shape of the interaction potential, nor did it affect the microstructure of the monolayer.

Conversely, adding only trace amounts of an ionic liquid [trihexyltetradecylphosphonium decanoate, IL (molecular structure in Fig. S7 [50])] to the hexadecane had a striking effect on the interparticle interaction potential and the resulting structure of the monolayers [Figs. 3(a)–3(d)].

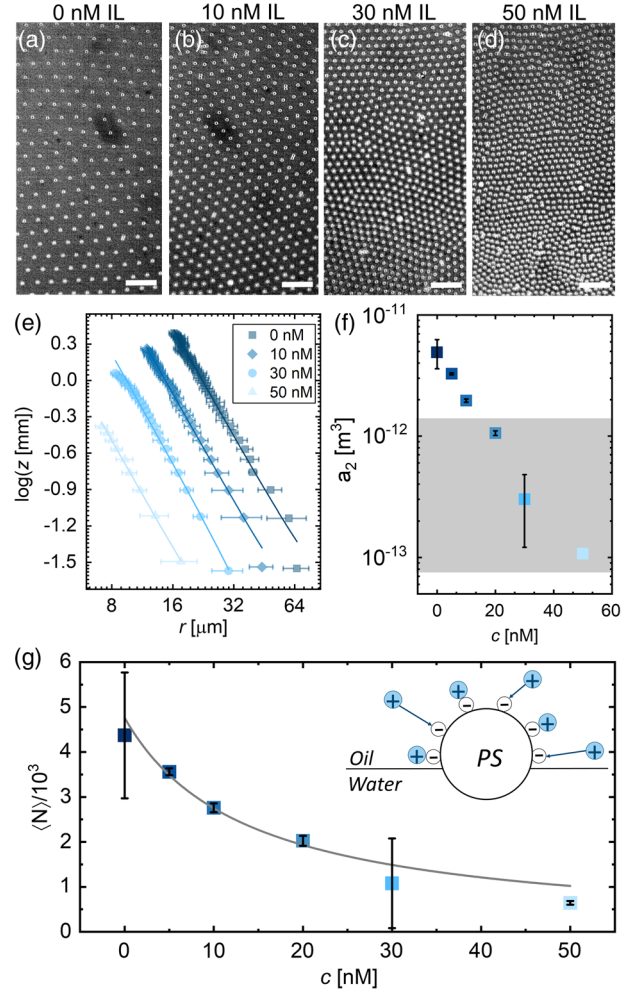


FIG. 3. The effect of adding IL to the organic phase. (a)–(d) Representative dark-field images of the $d = 2.80 \mu\text{m}$ PS monolayers at the bottom of the experimental cell (i.e., $z \approx 0.1\text{--}0.3 \text{mm}$) for different IL concentrations. Scale bars: $20 \mu\text{m}$. (e) z vs r for different IL concentrations. Error bars show the standard deviation of r in height bins of $50 \mu\text{m}$. (f) a_2 as a function of the concentration of IL c . The gray area marks the range of values reported in literature [31–34,41]. (g) Average number of charges at the particle-oil interface $\langle N \rangle$ as a function of c . Line indicates the fit to Eq. (5). Error bars in (f) and (g) indicate the error measured over 3 independent experiments. Inset: Sketch of the adsorption of positive ions of the organic electrolyte to the negative charges on the particle surface exposed to the oil side.

The plots of z vs r shown in Fig. 3(e) reveal a shift towards smaller interparticle distances with increasing amount of IL at the same z , while retaining an overall similar functional form, indicating that the magnitude of the dipolar interactions is strongly affected by progressively introducing minute amounts of the IL into the organic phase. The values of a_2 , plotted as a function of the concentration of ionic liquid c [Fig. 3(f)] clearly show that the strength of the interaction potential decreases over roughly 2 orders of magnitude by increasing c from 0 to 50 nM (Fig. 3). At $c = 50$ nM, small aggregates in the denser region of the particle monolayer start to appear [Fig. 3(d)], while for $c > 50$ nM all particles aggregate into fractal-like structures (Fig. S8 [50]). This indicates that, under gravity and beyond 50 nM IL, the repulsive component of the potential reaches a magnitude that is comparable to the attractive capillary force arising from out-of-plane undulations of the contact lines on the particles [20], causing the particles to aggregate. Setting our extracted repulsive dipolar potential at 50 nM IL equal to the attractive capillary potential [55–57] (i.e., $(a_2 k_B T / r^3) = 12\pi\gamma H^2 \{ [d \sin(\theta)^4] / 2r^4 \}$ with γ being the interfacial tension) for a minimum distance observed before aggregation of $r \approx 7$ μm , we estimate an amplitude of the contact angle undulations $H \approx 35$ nm, which is comparable to literature values [57].

Previous work by Danov, Kralchevsky, and others [40,57] quantified the electrostatic dipolar interaction energy between two floating particles at a fluid-fluid interface as

$$U(r) = \frac{p_d^2}{2\epsilon_0\epsilon_n r^3}, \quad (4)$$

where ϵ_n is the dielectric constant of the nonpolar phase, and ϵ_0 is the permittivity of vacuum. The parameter p_d is the effective dipole moment of the particle, which is $p_d = 1/2\pi\sigma D(\theta, \epsilon_{pn})d^3 \sin^3(\theta)$, with σ being the surface charge density at the particle or nonpolar fluid interface, and $D(\theta, \epsilon_{pn})$ a tabulated dimensionless function [40] that depends on the contact angle of the particles θ , as well as the ratio of the dielectric constants of the particle and nonpolar fluid ϵ_{pn} [50].

Considering the minute amounts of added IL, it is reasonable to assume that ϵ_n remains unchanged. We also note that with the added ionic liquid, the estimated Debye length κ^{-1} ranges from 220 to 700 nm, yielding $\kappa r > 10$, and therefore the screening remains insignificant [29]. Furthermore, we do not find any changes in θ due to the addition of IL (Fig. S3 [50]), suggesting that the modulation of the interaction potential directly results from changes in σ . Similarly, but in the opposite direction to the case of charge regulation observed in systems of charged colloids in nonpolar solvents [58–63], we assume our system to obey an associative discharging mechanism in which a single charged group on the particle surface

S^- can be occupied by a positive IL ion P^+ . In this frame of reference, our system is expected to obey Langmuir-type adsorption that relates the average number of unoccupied charges at the particle-oil interface $\langle N \rangle$ to the total number of sites available for adsorption $\langle N \rangle_0$ [64]:

$$\langle N \rangle = \frac{\langle N \rangle_0}{1 + K/c}, \quad (5)$$

where K is a constant that depends on the equilibrium constant of the reaction $S^- + P^+ \rightleftharpoons SP$ and the surface potential. For our particles, we find $D(\theta, \epsilon_{pn}) \approx 1.05$ [40]. Substituting the latter into Eq. (4), we are able to calculate σ , from which we directly derive the average number of charged groups per particle exposed to the oil $\langle N \rangle$ [50]. Figure 3(g) shows the calculated values of $\langle N \rangle$ as a function of c . In the absence of any IL we find $\langle N \rangle \approx 5000$. Dividing the surface area of the particle by the number of charges, we find that we have an area of ≈ 3000 nm² per charged group, which is in good agreement with previous literature [29,35]. When introducing the IL, we find that our $\langle N \rangle$ vs r data are well described by Eq. (5), as indicated by the fitted line in Fig. 3(g). We extract a value for the association parameter of the particles of $K = 1.4 \times 10^8 \pm 2.6 \times 10^6$. Similar trends are observed for the particles with $d = 2.48$ and $d = 2.07$ μm , with a lower value of K for the less charged colloids (see Fig. S9 [50]).

In conclusion, we have shown that introducing nanomolar amounts of an organic salt into the nonpolar phase allows for a continuous control over the strength of the repulsive dipolar interaction potential between charged polystyrene spheres confined at a water-oil interface. Our results strongly suggest that charge regulation by means of an associative discharging mechanism is responsible for modulating the interaction potential over 2 orders of magnitude upon adding the IL. These findings underline that the presence of even ultralow amounts of oil-soluble impurities might affect the measured interactions between adsorbed particles at fluid interfaces. Differently from previous works, which have investigated lateral and normal interparticle interactions for particles progressively breaching the fluid interface [65,66], we focus on monolayers of colloids that are “instantly” brought to the interface by solvent-assisted spreading and evaluate their interaction after long equilibration times. However, we envision that the addition of IL may also affect the kinetics of the spontaneous adsorption of particles to the interface and lead to modifications of the normal interactions between particles close to or at an interface [47,67]. Our results, moreover, offer an alternative perspective into which factors can be used to tailor the assembly of charged particles at a water-nonpolar fluid interface without the experimentally demanding use of external fields. This novel approach is envisioned to prove versatile and adaptable, with interesting implications for processes such

as emulsion destabilization or for fundamental studies on 2D crystallization.

The authors thank Svetoslav Anachov, Eric Dufresne, Jan Vermant, Martin Oettel, and Alvaro Dominiguez for inspiring discussions and Federico Paratore for support. The authors would also like to thank Job Thijssen and the referees for useful input and suggestions to the manuscript. C. v. B. acknowledges funding from the European Union's Horizon 2020 MSCA-ITN-ETN, project No. 812780. J. V. acknowledges funding from the European Union's Horizon 2020 research and innovation programme under the Marie Skłodowska Curie Grant Agreement No. 888076.

Author contributions are defined based on the CRediT (contributor roles taxonomy) and listed alphabetically. Conceptualization: C. v. B., L. I., J. V.; Formal analysis: C. v. B., L. I.; Funding acquisition: L. I., J. V.; Investigation: C. v. B.; Methodology: C. v. B., L. I., J. V.; Project administration: L. I., J. V.; Software: C. v. B.; Supervision: L. I.; Validation: C. v. B.; Visualization: C. v. B., L. I., J. V.; Writing, original draft: C. v. B., L. I., J. V.; Writing, review, and editing: C. v. B., L. I., J. V. The authors declare that they have no known competing financial interests or personal relationships that could have appeared to influence the work reported in this letter.

*Present address: Department of Chemistry and CSGI, University of Florence, via della Lastruccia 3, Sesto Fiorentino, I-50019 Firenze, Italy.

†lucio.isa@mat.ethz.ch

- [1] L. Tran and M. F. Haase, Templating interfacial nanoparticle assemblies via in Situ techniques, *Langmuir* **35**, 8584 (2019).
- [2] N. Vogel, M. Retsch, C.-A. Fustin, A. del Campo, and U. Jonas, Advances in colloidal assembly: The design of structure and hierarchy in two and three dimensions, *Chem. Rev.* **115**, 6265 (2015).
- [3] C. Eisenmann, P. Keim, U. Gasser, and G. Maret, Melting of anisotropic colloidal crystals in two dimensions, *J. Phys. Condens. Matter* **16**, S4095 (2004).
- [4] C. Eisenmann, P. Keim, U. Gasser, and G. Maret, Anisotropic Defect-Mediated Melting of Two-Dimensional Colloidal Crystals, *Phys. Rev. Lett.* **93**, 105702 (2004).
- [5] H. H. von Grünberg, P. Keim, K. Zahn, and G. Maret, Elastic Behavior of a Two-Dimensional Crystal Near Melting, *Phys. Rev. Lett.* **93**, 255703 (2004).
- [6] P. Keim, G. Maret, U. Herz, and H. H. von Grünberg, Harmonic Lattice Behavior of Two-Dimensional Colloidal Crystals, *Phys. Rev. Lett.* **92**, 215504 (2004).
- [7] W. T. M. Irvine, V. Vitelli, and P. M. Chaikin, Pleats in crystals on curved surfaces, *Nature (London)* **468**, 947 (2010).
- [8] J. Vialletto and M. Anyfantakis, Exploiting additives for directing the adsorption and organization of colloid particles at fluid interfaces, *Langmuir* **37**, 9302 (2021).
- [9] S. Reynaert, P. Moldenaers, and J. Vermant, Control over colloidal aggregation in monolayers of latex particles at the oil-water interface, *Langmuir* **22**, 4936 (2006).
- [10] S. Srivastava, D. Nykypanchuk, M. Fukuto, and O. Gang, Tunable nanoparticle arrays at charged interfaces, *ACS Nano* **8**, 9857 (2014).
- [11] G. Li-Destri, R. Ruffino, N. Tuccitto, and G. Marletta, In situ structure and force characterization of 2D nano-colloids at the air/water interface, *Soft Matter* **15**, 8475 (2019).
- [12] S. Reynaert, P. Moldenaers, and J. Vermant, Interfacial rheology of stable and weakly aggregated two-dimensional suspensions, *Phys. Chem. Chem. Phys.* **9**, 6463 (2007).
- [13] D. Truzzolillo, H. Sharaf, U. Jonas, B. Loppinet, and D. Vlassopoulos, Tuning the structure and rheology of polystyrene particles at the air-water interface by varying the pH, *Langmuir* **32**, 6956 (2016).
- [14] M. Anyfantakis, J. Vialletto, A. Best, G. K. Auernhammer, H.-J. Butt, B. P. Binks, and D. Baigl, Adsorption and crystallization of particles at the air-water interface induced by minute amounts of surfactant, *Langmuir* **34**, 15526 (2018).
- [15] J. Vialletto, S. Rudiuk, M. Morel, and D. Baigl, From bulk crystallization of inorganic nanoparticles at the air/water interface: Tunable organization and intense structural colors, *Nanoscale* **12**, 6279 (2020).
- [16] A. Snezhko and I. S. Aranson, Magnetic manipulation of self-assembled colloidal asters, *Nat. Mater.* **10**, 698 (2011).
- [17] J. Vialletto, M. Anyfantakis, S. Rudiuk, M. Morel, and D. Baigl, Photoswitchable dissipative two-dimensional colloidal crystals, *Angew. Chem., Int. Ed.* **58**, 9145 (2019).
- [18] J. Vialletto, S. Rudiuk, M. Morel, and D. Baigl, Photothermally reconfigurable colloidal crystals at a fluid interface, a generic approach for optically tunable lattice properties, *J. Am. Chem. Soc.* **143**, 11535 (2021).
- [19] M. Oettel and S. Dietrich, Colloidal interactions at fluid interfaces, *Langmuir* **24**, 1425 (2008).
- [20] T. S. Horozov, R. Aveyard, J. H. Clint, and B. Neumann, Particle zips: Vertical emulsion films with particle monolayers at their surfaces, *Langmuir* **21**, 2330 (2005).
- [21] V. Garbin, J. C. Crocker, and K. J. Stebe, Nanoparticles at fluid interfaces: Exploiting capping ligands to control adsorption, stability and dynamics, *J. Colloid Interface Sci.* **387**, 1 (2012).
- [22] P. A. Kralchevsky and K. Nagayama, Capillary interactions between particles bound to interfaces, liquid films and biomembranes, *Adv. Colloid Interface Sci.* **85**, 145 (2000).
- [23] J. Vialletto, M. Zanini, and L. Isa, Attachment and detachment of particles to and from fluid interfaces, *Curr. Opin. Colloid Interface Sci.* **58**, 101560 (2022).
- [24] I. Muntz, F. Waggett, M. Hunter, A. B. Schofield, P. Bartlett, D. Marenduzzo, and J. H. J. Thijssen, Interaction between nearly hard colloidal spheres at an oil-water interface, *Phys. Rev. Res.* **2**, 023388 (2020).
- [25] R. Aveyard, J. H. Clint, D. Nees, and V. N. Paunov, Compression and structure of monolayers of charged latex particles at air/water and octane/water interfaces, *Langmuir* **16**, 1969 (2000).
- [26] T. S. Horozov, R. Aveyard, J. H. Clint, and B. P. Binks, Order-disorder transition in monolayers of modified

- monodisperse silica particles at the octane-water interface, *Langmuir* **19**, 2822 (2003).
- [27] P. Pieranski, Two-Dimensional Interfacial Colloidal Crystals, *Phys. Rev. Lett.* **45**, 569 (1980).
- [28] L. J. Bonales, J. E. F. Rubio, H. Ritacco, C. Vega, R. G. Rubio, and F. Ortega, Freezing transition and interaction potential in monolayers of microparticles at fluid interfaces, *Langmuir* **27**, 3391 (2011).
- [29] A. J. Hurd, The electrostatic interaction between interfacial colloidal particles, *J. Phys. A* **18**, L1055 (1985).
- [30] B. J. Park, J. P. Pantina, E. M. Furst, M. Oettel, S. Reynaert, and J. Vermant, Direct measurements of the effects of salt and surfactant on interaction forces between colloidal particles at water-oil interfaces, *Langmuir* **24**, 1686 (2008).
- [31] B. J. Park, J. Vermant, and E. M. Furst, Heterogeneity of the electrostatic repulsion between colloids at the oil–water interface, *Soft Matter* **6**, 5327 (2010).
- [32] B. J. Park and E. M. Furst, Attractive interactions between colloids at the oil–water interface, *Soft Matter* **7**, 7676 (2011).
- [33] B. J. Park, B. Lee, and T. Yu, Pairwise interactions of colloids in two-dimensional geometric confinement, *Soft Matter* **10**, 9675 (2014).
- [34] K. Masschaele, B. J. Park, E. M. Furst, J. Fransaer, and J. Vermant, Finite Ion-Size Effects Dominate the Interaction between Charged Colloidal Particles at an Oil-Water Interface, *Phys. Rev. Lett.* **105**, 048303 (2010).
- [35] R. Aveyard, B. P. Binks, J. H. Clint, P. D. I. Fletcher, T. S. Horozov, B. Neumann, V. N. Paunov, J. Annesley, S. W. Botchway, D. Nees, A. W. Parker, A. D. Ward, and A. N. Burgess, Measurement of Long-Range Repulsive Forces between Charged Particles at an Oil-Water Interface, *Phys. Rev. Lett.* **88**, 246102 (2002).
- [36] L. Parolini, A. D. Law, A. Maestro, D. M. A. Buzza, and P. Cicuta, Interaction between colloidal particles on an oil–water interface in dilute and dense phases, *J. Phys. Condens. Matter* **27**, 194119 (2015).
- [37] D.-G. Lee, P. Cicuta, and D. Vella, Self-assembly of repulsive interfacial particles via collective sinking, *Soft Matter* **13**, 212 (2017).
- [38] P. V. Petkov, K. D. Danov, and P. A. Kralchevsky, Surface pressure isotherm for a monolayer of charged colloidal particles at a water/nonpolar-fluid interface: experiment and theoretical model, *Langmuir* **30**, 2768 (2014).
- [39] V. N. Paunov, Novel method for determining the three-phase contact angle of colloid particles adsorbed at air-water and oil-water interfaces, *Langmuir* **19**, 7970 (2003).
- [40] K. D. Danov and P. A. Kralchevsky, Electric forces induced by a charged colloid particle attached to the water–nonpolar fluid interface, *J. Colloid Interface Sci.* **298**, 213 (2006).
- [41] C. L. Wirth, E. M. Furst, and J. Vermant, Weak electrolyte dependence in the repulsion of colloids at an oil–water interface, *Langmuir* **30**, 2670 (2014).
- [42] M. F. Hsu, E. R. Dufresne, and D. A. Weitz, Charge stabilization in nonpolar solvents, *Langmuir* **21**, 4881 (2005).
- [43] G. N. Smith, J. E. Hallett, and J. Eastoe, Celebrating *Soft Matter*’s 10th anniversary: Influencing the charge of poly (methyl methacrylate) latexes in nonpolar solvents, *Soft Matter* **11**, 8029 (2015).
- [44] M. E. Leunissen, A. van Blaaderen, A. D. Hollingsworth, M. T. Sullivan, and P. M. Chaikin, Electrostatics at the oil–water interface, stability, and order in emulsions and colloids, *Proc. Natl. Acad. Sci. U.S.A.* **104**, 2585 (2007).
- [45] A. Yethiraj and A. van Blaaderen, A colloidal model system with an interaction tunable from hard sphere to soft and dipolar, *Nature (London)* **421**, 513 (2003).
- [46] N. A. Elbers, J. E. S. van der Hoeven, D. A. M. de Winter, C. T. W. M. Schneijdenberg, M. N. van der Linden, L. Filion, and A. van Blaaderen, Repulsive van der Waals forces enable Pickering emulsions with non-touching colloids, *Soft Matter* **12**, 7265 (2016).
- [47] J. C. Everts, S. Samin, and R. V. Roij, Tuning Colloid-Interface Interactions by Salt Partitioning, *Phys. Rev. Lett.* **117**, 098002 (2016).
- [48] A. D. Law, D. M. A. Buzza, and T. S. Horozov, Two-Dimensional Colloidal Alloys, *Phys. Rev. Lett.* **106**, 128302 (2011).
- [49] T. Sakka, D. Kozawa, K. Tsuchiya, N. Sugiman, G. Øye, K. Fukami, N. Nishi, and Y. H. Ogata, Two-dimensional array of particles originating from dipole–dipole interaction as evidenced by potential curve measurements at vertical oil/water interfaces, *Phys. Chem. Chem. Phys.* **16**, 16976 (2014).
- [50] See Supplemental Material at <http://link.aps.org/supplemental/10.1103/PhysRevLett.131.128202> for experimental details, supporting data and detailed derivations.
- [51] J. C. Crocker and D. G. Grier, Methods of digital video microscopy for colloidal studies, *J. Colloid Interface Sci.* **179**, 298 (1996).
- [52] A. Maestro, L. J. Bonales, H. Ritacco, R. G. Rubio, and F. Ortega, Effect of the spreading solvent on the three-phase contact angle of microparticles attached at fluid interfaces, *Phys. Chem. Chem. Phys.* **12**, 14115 (2010).
- [53] K. Dietrich, G. Volpe, M. N. Sulaiman, D. Renggli, I. Buttinoni, and L. Isa, Active Atoms and Interstitials in Two-Dimensional Colloidal Crystals, *Phys. Rev. Lett.* **120**, 268004 (2018).
- [54] D. Frydel, S. Dietrich, and M. Oettel, Charge Renormalization for Effective Interactions of Colloids at Water Interfaces, *Phys. Rev. Lett.* **99**, 118302 (2007).
- [55] D. Stamou, C. Duschl, and D. Johannsmann, Long-range attraction between colloidal spheres at the air-water interface: The consequence of an irregular meniscus, *Phys. Rev. E* **62**, 5263 (2000).
- [56] P. A. Kralchevsky and N. D. Denkov, Capillary forces and structuring in layers of colloid particles, *Curr. Opin. Colloid Interface Sci.* **6**, 383 (2001).
- [57] P. A. Kralchevsky, K. D. Danov, and P. V. Petkov, Soft electrostatic repulsion in particle monolayers at liquid interfaces: Surface pressure and effect of aggregation, *Phil. Trans. R. Soc. A* **374**, 20150130 (2016).
- [58] C. P. Royall, M. E. Leunissen, A.-P. Hynninen, M. Dijkstra, and A. van Blaaderen, Re-entrant melting and freezing in a model system of charged colloids, *J. Chem. Phys.* **124**, 244706 (2006).
- [59] J. C. Everts, N. Boon, and R. van Roij, Density-induced reentrant melting of colloidal Wigner crystals, *Phys. Chem. Chem. Phys.* **18**, 5211 (2016).

- [60] J. E. Hallett, D. A. Gillespie, R. M. Richardson, and P. Bartlett, Charge regulation of nonpolar colloids, *Soft Matter* **14**, 331 (2018).
- [61] G. Hussain, A. Robinson, and P. Bartlett, Charge generation in low-polarity solvents: Poly (ionic liquid)-functionalized particles, *Langmuir* **29**, 4204 (2013).
- [62] G. Seth Roberts, T. A. Wood, W. J. Frith, and P. Bartlett, Direct measurement of the effective charge in nonpolar suspensions by optical tracking of single particles, *J. Chem. Phys.* **126**, 194503 (2007).
- [63] F. Strubbe, F. Beunis, M. Marescaux, and K. Neyts, Charging mechanism in colloidal particles leading to a linear relation between charge and size, *Phys. Rev. E* **75**, 031405 (2007).
- [64] B. W. Ninham and V. A. Parsegian, Electrostatic potential between surfaces bearing ionizable groups in ionic equilibrium with physiologic saline solution, *J. Theor. Biol.* **31**, 405 (1971).
- [65] L. Helden, K. Dietrich, and C. Bechinger, Interactions of colloidal particles and droplets with water–oil interfaces measured by total internal reflection microscopy, *Langmuir* **32**, 13752 (2016).
- [66] A. Wang, J. W. Zwanikken, D. M. Kaz, R. McGorty, A. M. Goldfain, W. B. Rogers, and V. N. Manoharan, Before the breach: Interactions between colloidal particles and liquid interfaces at nanoscale separations, *Phys. Rev. E* **100**, 042605 (2019).
- [67] H. M. Lee, Y. W. Kim, E. M. Go, C. Revadekar, K. H. Choi, Y. Cho, S. K. Kwak, and B. J. Park, Direct measurements of the colloidal Debye force, *Nat. Commun.* **14**, 3838 (2023).